# Comparison Between Theoretical and Experimental Deformation Density of 1,3,5,7-Tetra-*t*-butyl-*s*-indacene

Yu Wang* ( 王 瑜 ) and Chih-Chieh Wang ( 王志傑 )
*Department of Chemistry, National Taiwan University Taipei, Taiwan*

1,3,5,7-Tetra-*t*-butyl-*s*-indacene is a twelve-membered fused-ring compound; the stabilization of the compound by bulky *t*-butyl groups is discussed. The distribution of bonding electron density is depicted in terms of deformation density using the experimental X-X method, a multipole expansion model and a calculation according to the extended Hückel molecular orbital method (EHMO). The molecules crystallize according to the space group $P2_1/n$ with cell parameters a = 9.700(3), b = 11.746(3), c = 10.858(2)Å, $\beta$ = 107.67(2)°, Z = 2 at 100K. The molecule has a center of inversion($\bar{1}$) and belongs to the symmetry point group $C_i$. The packing of two unique *t*-butyl groups in the asymmetric unit appears significantly different. However, the map of deformation density in the plane of the ring shows pseudo $D_{2h}$ symmetry. The accumulation of density at the midpoint of the bonds is observed as expected. The theoretical deformation densities agree with the experimental ones. Analyses of the molecular-orbital wavefunctions provide a good illustration of the aromatic $\pi$-electron system. A theoretical study of a series of substituents (-H, -$CH_3$, -*t*-butyl) on *s*-indacene illustrates the stabilization effect of the *t*-butyl group on the 12-$\pi$-electron ring system.

## INTRODUCTION

*s*-Indacene is a thermally unstable molecule having 12-$\pi$ electrons. However, 1,3,5,7-tetra-alkyl-*s*-indacenes are relatively stable, especially with bulky *t*-butyl groups. That $^{13}C$ NMR spectra showed no temperature dependence of the line shape down to -130°C[1] indicates that either the $\pi$-electron system of the 12-membered ring is completely delocalized (**1C**) or only a small energy barrier exists between the two valence isomers (**1A** and **1B**). We have performed a detailed study of the distribution of charge density in 1,3,5,7-tetra-*t*-butyl-*s*-indacene to understand whether the bulky substituents affect the electron distribution of such a 12-$\pi$-electron system. The structure[1] at room temperature shows a pseudo-$D_{2h}$ molecular symmetry of the geometry of the 12-membered ring. A detailed analysis of anisotropic displacement parameters (ADP)[2] of the carbon atoms of this compound gave no evidence of disorder, i.e. no indication of resonance between valence isomers. A transition state of the valence isomerization was proposed for the molecular structure in the crystal.[2] We have investigated this state in terms of molecular-orbital wavefunctions.

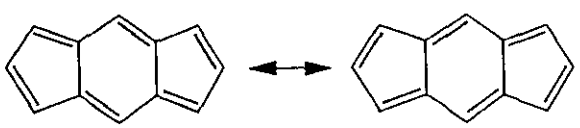

1A 1B

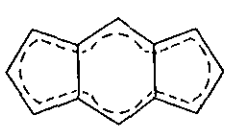

1C

## EXPERIMENTAL SECTION

A single crystal of size 0.14 x 0.27 x 0.36 mm was selected for measurements of diffraction data at 100K, using a CAD4 diffractometer equipped with a graphite monochromator. Mo K$\alpha$ radiation was used for the intensity measurements; a unique set was collected up to $2\theta$ = 84°. An additional symmetry-equivalent set was collected up to $2\theta$ = 72°. Furthermore, seven measurements with different $\psi$ values for each reflection up to $2\theta$ = 32° and one extra measurement with $\psi$ = 15° for reflections with 32° ≤ $2\theta$ ≤ 72° were collected. This process yielded 22,668 meas-

Dedicated to Professor Yau-Tang Lin ( 林耀堂 ) on the occasion of his eightieth birthday.

urements in total, leading to 5675 unique reflections after averaging of the equivalents. The interest agreement index $\Sigma\Delta I_i/\Sigma I_i$ is 0.02. 4383 reflections were considered observed ($F_o > 4\sigma(F_o)$). Cell parameters were obtained by least-squares fit of 75 reflections in the range $16° \leq 2\theta \leq 40°$. The structure was refined by full-matrix least squares. The final agreement indices were $R(F) = 0.043$, $R_w(F) = 0.039$ in which $w = 4F_o^2/[\sigma^2(I) + (0.01I_{net})^2]$. Positional and thermal parameters of all atoms except H1 and H5 used for calculation of the deformation density maps were obtained from high-order ($\sin\theta/\lambda > 0.65Å^{-1}$) refinement $F^{calc/HO}$; the hydrogen-atom coordinates for H1 and H5 were set by extension of the C-H vectors until the C-H distances reached 1.085 Å. Maps of the experimental deformation density $\Delta\rho_{x-x}$ were calculated from diffraction data with $\sin\theta/\lambda \leq 0.75Å^{-1}$; $\Delta\rho_{x-x} = \rho^{obs} - \rho^{calc/HO}$ and the electron density $\rho$ is the Fourier transform of the corresponding structural amplitudes, $F_h$

$$\text{i.e.} \quad \rho^{obs}_{(r)} = \frac{1}{V}\sum_{\underset{\sim}{h}} F^{obs}_{\underset{\sim}{h}} \exp 2\pi i(\underset{\sim}{h} \cdot \underset{\sim}{r})$$

The MO calculation was carried out using the coordinates obtained from the diffraction data at 100K . The deformation density was computed by subtraction of the sum of spherical atomic densities (e.g. $s^2p_x^{2/3}p_y^{2/3}p_z^{2/3}$ for C) from the total electron density of the occupied molecular orbitals. The sum of spherical atomic densities is calculated with atoms at the same nuclear positions as the equilibrium molecular geometry.

$$\text{i.e.} \quad \Delta\rho_{theo} = \sum_{i=1}^{HOMO} \rho_i^{MO} - \sum_j \rho_j^{atom}$$

The EHMO calculation was done with the ICON[4] program. For the density calculation MOPLOT[4] and a locally developed routine[5] for contour plots were used.

In addition, an electron-density distribution $\Delta\rho_{M-A}$ based on a multipole model was calculated in order to obtain further information. Basically, this distribution resembles the experimental one $\Delta\rho_{x-x}$, except that $\rho^{obs}$ was replaced by $\rho^{multipole}$, such that

$$\rho^{multipole} = \rho^{core} + P_v\rho^{val} + \sum_{l=0}^{l}\sum_{m=-l}^{l} P_{lm}R_l(r)Y_{lm}$$

The first two terms are the spherical part of the electron density for core and valence electrons respectively. The third term is the sum of the multipole expansion in terms of the spherical-harmonic series $Y_{lm}$. $P_v$ and $P_{lm}$ are population coefficients which were obtained by least-squares refinement[6] together with conventional positional and thermal parameters. The dynamic map has been calculated with the thermal vibrations of nuclei up to experimental resolution (Fig. 4a). An additional static map was further calculated without the thermal vibrations of the nuclei and up to infinite resolution (Fig. 4b), this map is comparable to the theoretically calculated ones.

## RESULTS AND DISCUSSION

The positional and anisotropic thermal parameters from the full data, high-order ($\geq 0.65Å^{-1}$) and multipole refinements are given in Tables 1 and 2[7]. The multipole coefficients, $P_{lm}$, are listed in Table 3. The bond distances and angles between the skeletal carbon atoms are shown in the schematic diagram (Fig. 1). The geometry is similar to that at room temperature[1], but the symmetry appears even closer to $D_{2h}$; that is, the differences between C1-C3* and C1-C2; C5-C6 and C5-C4; C2-C6 and C3-C4 are all smaller than those at room temperature and all within one standard error. Thus from the geometry of the ring skeleton, the symmetry is close to $D_{2h}$. Although the molecular symmetry may belong to $D_{2h}$, the packing of the two *t*-butyl groups in the solid is obviously different, as depicted in Fig. 2. There C7,C9-C11 groups are packed in an eclipsed form along the

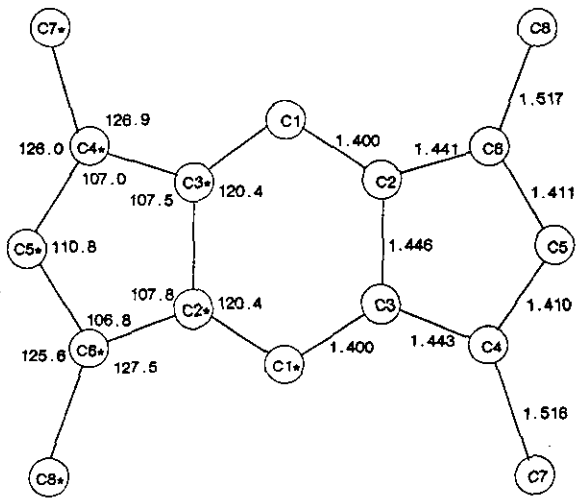


Fig. 1. Molecular structure of 1,3,5,7-*t*-butyl-*s*-indacene with bond distances (Å) and angles(°); the standard errors are 0.001Å and 0.3° respectively.

Table 1. Atomic Parameters x,y,z and Beq.($Å^2$) Estimated Standard Errors in Parentheses Refer to the Last Digit Printed

| | x | y | z | Beq | | x | y | z | Beq |
|---|---|---|---|---|---|---|---|---|---|
| Cl a. | 0.38118(7) | 0.07183(6) | 0.50021(6) | 0.88(2) | H92 | 0.810 (1) | -0.0069 (8) | 0.088 (1) | 2.5 (2) |
| b. | 0.38096(6) | 0.07200(5) | 0.50018(5) | 0.79(1) | | 0.821 (7) | -0.012 (6) | 0.096 (6) | 2.9 (7) |
| c. | 0.38116(8) | 0.07183(7) | 0.50024(7) | 0.83(2) | | 0.812 | -0.008 | 0.088 | 2.3 |
| C2 | 0.43848(7) | 0.07466(5) | 0.39650(6) | 0.81(2) | H93 | 0.6382 (9) | 0.0120 (7) | 0.0395 (9) | 1.6 (2) |
| | 0.43849(5) | 0.07480(4) | 0.39654(5) | 0.75(1) | | 0.644 (6) | 0.024 (5) | 0.044 (5) | 2.5 (6) |
| | 0.43846(8) | 0.07473(6) | 0.39648(7) | 0.78(2) | | 0.638 | 0.012 | 0.039 | 1.5 |
| C3 | 0.55905(7) | 0.00231(5) | 0.39653(6) | 0.82(2) | H101 | 0.606 (1) | -0.1691 (8) | 0.1549 (9) | 2.1 (2) |
| | 0.55908(5) | 0.00235(5) | 0.39655(5) | 0.74(1) | | 0.591 (9) | -0.177 (7) | 0.155 (8) | 3.3 (8) |
| | 0.55905(8) | 0.00227(7) | 0.39651(7) | 0.79(2) | | 0.605 | -0.171 | 0.154 | 2.2 |
| C4 | 0.59714(7) | 0.02729(6) | 0.28095(6) | 0.87(2) | H102 | 0.784 (1) | -0.1882 (8) | 0.2007 (9) | 2.3 (2) |
| | 0.59729(5) | 0.02714(5) | 0.28093(5) | 0.79(1) | | 0.817 (6) | -0.181 (5) | 0.215 (5) | 2.5 (6) |
| | 0.59729(8) | 0.02716(7) | 0.28096(7) | 0.83(2) | | 0.784 | -0.188 | 0.200 | 2.3 |
| C5 | 0.50050(7) | 0.11147(6) | 0.21332(6) | 0.98(2) | H103 | 0.694 (1) | -0.1934 (9) | 0.305 (1) | 2.9 (2) |
| | 0.50053(6) | 0.11167(5) | 0.21299(5) | 0.91(1) | | 0.684 (6) | -0.202 (5) | 0.301 (6) | 2.7 (6) |
| | 0.50045(9) | 0.11157(7) | 0.21309(7) | 0.94(2) | | 0.695 | -0.194 | 0.305 | 2.5 |
| C6 | 0.40241(7) | 0.14228(6) | 0.28023(6) | 0.89(2) | H111 | 0.869 (1) | -0.0380 (9) | 0.430 (1) | 2.5 (2) |
| | 0.40223(6) | 0.14230(5) | 0.28033(5) | 0.82(1) | | 0.877 (6) | -0.055 (5) | 0.445 (6) | 2.6 (6) |
| | 0.40234(8) | 0.14235(7) | 0.28052(7) | 0.84(2) | | 0.870 | -0.037 | 0.430 | 2.4 |
| C7 | 0.72065(7) | -0.02408(6) | 0.24100(6) | 1.01(2) | H112 | 0.950 (1) | -0.0301 (9) | 0.319 (1) | 2.5 (2) |
| | 0.72062(6) | -0.02406(5) | 0.24108(5) | 0.93(1) | | 0.948 (5) | -0.026 (4) | 0.310 (4) | 2.1 (5) |
| | 0.72055(8) | -0.02385(7) | 0.24098(7) | 0.97(2) | | 0.950 | -0.028 | 0.320 | 2.5 |
| C8 | 0.28250(7) | 0.22989(6) | 0.23621(6) | 1.11(2) | H113 | 0.876 (1) | 0.0868 (9) | 0.3590 (9) | 2.1 (2) |
| | 0.28251(7) | 0.22985(5) | 0.23610(6) | 1.03(1) | | 0.88 (1) | 0.093 (9) | 0.348 (9) | 4.0 (1) |
| | 0.28269(9) | 0.22983(7) | 0.23621(8) | 1.07(2) | | 0.878 | 0.087 | 0.361 | 2.6 |
| C9 | 0.72888(8) | 0.02741(7) | 0.11361(7) | 1.36(2) | H121 | 0.262 (1) | 0.2190 (9) | 0.0379 (9) | 2.4 (2) |
| | 0.72907(8) | 0.02762(6) | 0.11357(6) | 1.27(2) | | 0.278 (7) | 0.234 (6) | 0.047 (7) | 3.0 (7) |
| | 0.72921(9) | 0.02752(8) | 0.11368(8) | 1.32(3) | | 0.262 | 0.218 | 0.039 | 2.7 |
| C10 | 0.69985(9) | -0.15365(6) | 0.22319(8) | 1.53(3) | H122 | 0.368 (1) | 0.3201 (7) | 0.1045 (8) | 1.6 (2) |
| | 0.69989(9) | -0.15370(6) | 0.22327(7) | 1.46(2) | | 0.376 (6) | 0.312 (5) | 0.107 (5) | 2.5 (6) |
| | 0.7000 (1) | -0.15358(8) | 0.22331(9) | 1.52(3) | | 0.370 | 0.320 | 0.106 | 1.8 |
| C11 | 0.86492(8) | 0.00132(8) | 0.34600(7) | 1.58(3) | H123 | 0.202 (1) | 0.3385 (9) | 0.0783 (9) | 2.6 (2) |
| | 0.86515(7) | 0.00139(8) | 0.34625(7) | 1.48(2) | | 0.213 (6) | 0.323 (5) | 0.078 (5) | 2.5 (6) |
| | 0.86498(9) | 0.00107(9) | 0.34613(8) | 1.52(3) | | 0.200 | 0.339 | 0.078 | 3.1 |
| C12 | 0.27744(9) | 0.27953(7) | 0.10420(7) | 1.63(3) | H131 | 0.313 (1) | 0.3008 (9) | 0.422 (1) | 3.0 (2) |
| | 0.27734(9) | 0.27957(7) | 0.10410(7) | 1.52(2) | | 0.306 (8) | 0.308 (6) | 0.442 (7) | 3.0 (7) |
| | 0.2775 (1) | 0.27950(8) | 0.10445(9) | 1.59(3) | | 0.311 | 0.300 | 0.421 | 2.9 |
| C13 | 0.3083 (1) | 0.32860(7) | 0.33408(8) | 1.93(3) | H132 | 0.226 (1) | 0.3853 (9) | 0.302 (1) | 2.7 (2) |
| | 0.3083 (1) | 0.32880(7) | 0.33423(8) | 1.82(2) | | 0.23 (1) | 0.37 (1) | 0.32 (1) | 4.0 (1) |
| | 0.3085 (1) | 0.32849(9) | 0.3342 (1) | 1.89(4) | | 0.227 | 0.388 | 0.303 | 2.5 |
| C14 | 0.13503(8) | 0.17401(8) | 0.22201(9) | 1.92(3) | H133 | 0.405 (1) | 0.3657 (9) | 0.3450 (9) | 3.0 (2) |
| | 0.13478(8) | 0.17396(8) | 0.22224(9) | 1.80(2) | | 0.414 (8) | 0.363 (6) | 0.350 (7) | 3.1 (8) |
| | 0.1350 (1) | 0.1742 (1) | 0.2222 (1) | 1.84(3) | | 0.407 | 0.366 | 0.345 | 2.7 |
| H1 | 0.2991 (9) | 0.1241 (7) | 0.5010 (8) | 1.4 (2) | H141 | 0.132 (1) | 0.1448 (8) | 0.3084 (9) | 2.3 (2) |
| | 0.295 (4) | 0.126 (3) | 0.497 (4) | 1.7 (4) | | 0.130 (8) | 0.121 (7) | 0.307 (7) | 3.1 (8) |
| | 0.298 | 0.124 | 0.501 | 1.5 | | 0.129 | 0.144 | 0.308 | 2.6 |
| H5 | 0.5025 (9) | 0.1449 (8) | 0.1321 (9) | 1.6 (2) | H142 | 0.116 (1) | 0.1085 (9) | 0.159 (1) | 2.9 (2) |
| | 0.501 (6) | 0.145 (5) | 0.121 (6) | 2.6 (6) | | 0.112 (7) | 0.106 (6) | 0.164 (6) | 3.0 (7) |
| | 0.502 | 0.145 | 0.131 | 1.5 | | 0.115 | 0.107 | 0.158 | 3.0 |
| H91 | 0.747 (1) | 0.1131 (8) | 0.1233 (9) | 2.0 (2) | H143 | 0.058 (1) | 0.2317 (9) | 0.1901 (9) | 2.7 (2) |
| | 0.748 (7) | 0.109 (7) | 0.111 (6) | 2.9 (7) | | 0.054 (5) | 0.240 (4) | 0.183 (4) | 1.9 (4) |
| | 0.748 | 0.112 | 0.122 | 1.9 | | 0.055 | 0.231 | 0.190 | 2.5 |

$Beq = 8/3\,\pi^2\Sigma_{ij}U_{ij}a_i^*a_j^*a_ia_j$

[a] full data refinements [b] high angle ($> 0.65\ Å^{-1}$) refinements [c] multipole refinements

Table 2. Anisotropic Temperature Factors $U_{ij} \times 100$

| | $u_{11}$ | $u_{22}$ | $u_{33}$ | $u_{12}$ | $u_{13}$ | $u_{23}$ |
|---|---|---|---|---|---|---|
| Cl a. | 1.11(2) | 1.20(3) | 1.03(3) | 0.10(2) | 0.36(2) | 0.02(2) |
| b. | 1.06(2) | 1.11(2) | 0.87(2) | 0.18(1) | 0.34(1) | 0.11(1) |
| c. | 1.06(3) | 1.16(3) | 0.97(3) | 0.27(3) | 0.37(2) | 0.14(2) |
| C2 | 1.10(2) | 1.09(3) | 0.90(3) | 0.04(2) | 0.31(2) | 0.06(2) |
| | 1.02(2) | 1.04(2) | 0.80(2) | 0.11(1) | 0.31(1) | 0.11(1) |
| | 1.04(3) | 1.12(3) | 0.83(3) | 0.18(2) | 0.35(2) | 0.15(2) |
| C3 | 1.08(2) | 1.15(3) | 0.90(2) | -0.01(2) | 0.35(2) | -0.02(2) |
| | 0.99(2) | 1.05(2) | 0.81(2) | 0.12(1) | 0.32(1) | 0.09(1) |
| | 1.02(3) | 1.12(3) | 0.87(3) | 0.18(2) | 0.32(2) | 0.11(2) |
| C4 | 1.17(2) | 1.20(3) | 0.98(2) | -0.06(2) | 0.40(2) | -0.04(2) |
| | 1.06(2) | 1.12(2) | 0.87(2) | 0.07(1) | 0.37(1) | 0.06(1) |
| | 1.11(3) | 1.23(3) | 0.90(3) | 0.12(3) | 0.43(2) | 0.10(2) |
| C5 | 1.39(3) | 1.42(3) | 0.95(3) | 0.06(2) | 0.43(2) | 0.19(2) |
| | 1.29(2) | 1.31(2) | 0.91(2) | 0.17(1) | 0.44(1) | 0.23(1) |
| | 1.33(3) | 1.36(3) | 0.96(3) | 0.19(3) | 0.45(2) | 0.26(3) |
| C6 | 1.19(3) | 1.18(3) | 0.99(3) | 0.04(2) | 0.30(2) | 0.08(2) |
| | 1.11(2) | 1.11(2) | 0.91(2) | 0.14(1) | 0.31(1) | 0.16(1) |
| | 1.15(3) | 1.15(3) | 0.93(3) | 0.20(2) | 0.35(2) | 0.22(2) |
| C7 | 1.34(3) | 1.48(3) | 1.17(3) | 0.12(2) | 0.61(2) | 0.04(2) |
| | 1.21(2) | 1.36(2) | 1.09(2) | 0.13(1) | 0.54(1) | 0.06(1) |
| | 1.20(3) | 1.42(3) | 1.17(3) | 0.13(3) | 0.53(2) | 0.09(3) |
| C8 | 1.53(3) | 1.42(3) | 1.28(3) | 0.42(2) | 0.45(2) | 0.36(2) |
| | 1.45(2) | 1.29(2) | 1.20(2) | 0.39(2) | 0.45(1) | 0.32(1) |
| | 1.46(3) | 1.39(3) | 1.25(3) | 0.38(3) | 0.46(3) | 0.32(3) |
| C9 | 2.05(3) | 2.00(3) | 1.43(3) | 0.07(3) | 1.00(3) | 0.15(3) |
| | 1.95(2) | 1.86(2) | 1.33(2) | 0.09(2) | 0.96(2) | 0.19(2) |
| | 2.08(3) | 1.89(4) | 1.36(3) | 0.12(3) | 1.00(3) | 0.21(3) |
| C10 | 2.65(4) | 1.55(3) | 2.02(3) | 0.25(3) | 1.32(3) | -0.03(3) |
| | 2.56(3) | 1.39(2) | 1.99(3) | 0.22(2) | 1.30(2) | -0.05(2) |
| | 2.69(4) | 1.43(4) | 2.06(4) | 0.21(3) | 1.35(3) | -0.04(3) |
| C11 | 1.23(3) | 3.07(4) | 1.72(3) | 0.02(3) | 0.46(2) | 0.07(3) |
| | 1.13(2) | 2.86(3) | 1.62(2) | 0.04(2) | 0.42(2) | 0.05(2) |
| | 1.20(3) | 2.95(4) | 1.64(3) | 0.00(3) | 0.44(3) | 0.01(3) |
| C12 | 2.51(4) | 2.21(4) | 1.55(3) | 0.82(3) | 0.73(3) | 0.78(3) |
| | 2.36(3) | 2.07(3) | 1.42(2) | 0.76(2) | 0.69(2) | 0.80(2) |
| | 2.41(4) | 2.18(4) | 1.49(4) | 0.82(3) | 0.68(3) | 0.83(3) |
| C13 | 3.72(5) | 1.70(3) | 1.93(4) | 0.89(3) | 0.87(3) | -0.02(3) |
| | 3.61(4) | 1.53(2) | 1.80(3) | 0.81(2) | 0.84(2) | -0.04(2) |
| | 3.73(5) | 1.56(4) | 1.92(4) | 0.87(4) | 0.88(4) | -0.03(3) |
| C14 | 1.45(3) | 2.90(4) | 2.84(4) | 0.44(3) | 0.53(3) | 0.99(3) |
| | 1.27(2) | 2.73(3) | 2.77(3) | 0.40(2) | 0.50(2) | 1.02(3) |
| | 1.30(3) | 2.74(5) | 2.87(5) | 0.35(3) | 0.51(3) | 0.95(4) |

Anisotropic temperature factors are of the form
Temp = $\exp[-2\pi^2(h^2u_{11}a^{*2} + ... + 2hku_{12}a^*b^* + ...)]$
[a] full data refinements
[b] high angle ( > 0.65Å$^{-1}$) refinements
[c] multipole refinements

b-axis whereas the C8,C12-C14 groups are packed in a staggered form. These results are consistent with the analysis[2] of anisotropic displacement parameters with the libration of exocyclic C4-C7 bond much smaller than that of C6-C8 bond. Thus, the exact molecular symmetry in the crystal is $C_i$; in other words, the two in-plane twofold axes are not present. Nevertheless, from the examination of the map of deformation density (Fig. 3), one sees that the twofold axes along C5-C5* and C1-C1* still exist at a standard deviation of one contour level (0.1 e Å$^{-3}$), but the shape of the contour deviates slightly. Therefore we conclude that the intermolecular packing does not affect the symmetry of the electron distribution. All the bonding electron densities for C-C and C-H bonds are observed as expected,[3-5,8,9] with density accumulation at the midpoint of the bonds. The peak density is about 0.4 - 0.6 e Å$^{-3}$ for the C-C bond and 0.2 - 0.3 e Å$^{-3}$ for the C-H bond. The agreement indices of the various refinements are listed in Table 4. The multipole expansion evidently improves the agreement. The distribution of deformation density according to the dynamic multipole model shown in Fig. 4a agrees with the experimental one (Fig. 3). The map of the deformation density according to the static multipole model (Fig. 4b) has essentially the same features as that in the dynamic case except that all the peak densities are increased; this result is expected when the vibrational motions of the nuclei are ignored. The net

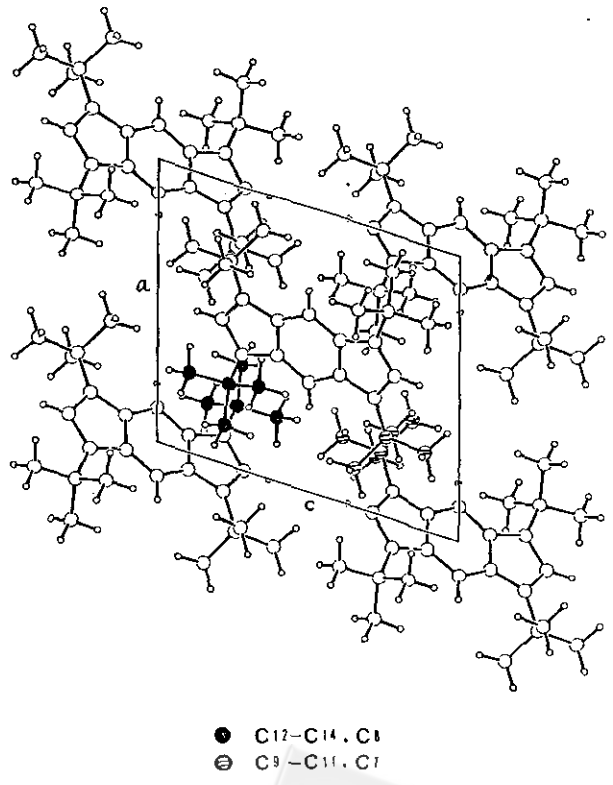


Fig. 2. Packing diagram with projection on b-axis.

Table 3. Atomic Multipole Coefficients ($P_{lm}$) of All Atoms

| Atom | | C(5) | C(6) | C(2) | C(3) | C(4) |
|---|---|---|---|---|---|---|
| k | HF | 0.982(2) | | | | |
| H | l=0,m= 0 | 4.40(4) | 4.20(3) | 4.24 (3) | 4.22 (3) | 4.17(3) |
| | l=0,m= 1 | -0.07(2) | -0.02(1) | -0.01 (1) | -0.02 (1) | 0.01(1) |
| | m= -1 | 0.06(2) | -0.04(1) | 0.04 (1) | 0.02 (1) | -0.02(1) |
| | m= 0 | 0.01(1) | 0.00(1) | -0.01 (1) | 0.00 (1) | -0.02(1) |
| | l=2,m= 0 | -0.19(1) | -0.22(1) | -0.18 (1) | -0.18 (1) | -0.24(1) |
| | m= 1 | 0.01(1) | 0.03(1) | 0.00 (1) | 0.00 (1) | -0.02(1) |
| | m= -1 | -0.05(1) | 0.01(1) | 0.04 (1) | 0.03 (1) | 0.00(1) |
| | m= 2 | -0.04(2) | -0.01(2) | 0.00 (2) | -0.08 (2) | 0.00(2) |
| | m= -2 | -0.03(2) | -0.01(1) | -0.03 (1) | -0.04 (2) | -0.04(1) |
| | l=3,m= 0 | 0.00(1) | 0.00(1) | 0.02 (1) | -0.02 (1) | 0.01(1) |
| | m= 1 | 0.03(1) | 0.04(1) | 0.00 (1) | 0.03 (1) | 0.01(1) |
| | m= -1 | 0.02(1) | -0.02(1) | 0.02 (1) | 0.01 (1) | 0.00(1) |
| | m= 2 | 0.00(1) | 0.00(1) | -0.01 (1) | -0.02 (1) | 0.01(1) |
| | m= -2 | -0.02(1) | -0.02(1) | 0.02 (1) | -0.02 (1) | 0.01(1) |
| | m= 3 | 0.26(2) | 0.27(1) | 0.29 (1) | 0.27 (2) | 0.27(1) |
| | m= -3 | -0.03(2) | -0.08(2) | -0.06 (2) | -0.12 (2) | -0.07(2) |
| Atom | | C(1) | C(7) | C(8) | C(9) | C(10) |
| H | l=0,m= 0 | 4.38(3) | 4.11(3) | 4.16 (3) | 4.72 (3) | 4.75(3) |
| | l=0,m= 1 | -0.06(1) | -0.05(1) | -0.06 (1) | -0.08 (1) | -0.11(1) |
| | m= -1 | -0.11(2) | -0.06(1) | 0.00 (1) | 0.00 (1) | -0.02(1) |
| | m= 0 | 0.01(1) | 0.02(1) | 0.01 (1) | -0.03 (1) | -0.01(1) |
| | l=2,m= 0 | -0.21(1) | 0.00(1) | -0.02 (2) | -0.09 (1) | 0.00(1) |
| | m= 1 | 0.00(1) | 0.03(1) | -0.01 (1) | 0.01 (1) | 0.02(1) |
| | m= -1 | 0.02(1) | -0.02(1) | 0.03 (1) | 0.05 (1) | -0.04(1) |
| | m= 2 | -0.09(2) | -0.02(1) | -0.03 (1) | -0.01 (1) | 0.02(1) |
| | m= -2 | 0.06(2) | 0.04(1) | 0.00 (1) | 0.04 (1) | 0.00(1) |
| | l=3,m= 0 | 0.04(1) | -0.04(2) | 0.00 (2) | 0.02 (1) | -0.01(1) |
| | m= 1 | 0.01(1) | -0.13(1) | -0.18 (1) | -0.15 (1) | -0.15(1) |
| | m= -1 | 0.01(1) | -0.20(1) | 0.23 (1) | 0.11 (1) | 0.10(1) |
| | m= 2 | 0.03(1) | 0.00(1) | -0.04 (1) | -0.01 (1) | 0.00(1) |
| | m= -2 | -0.01(1) | -0.02(1) | 0.02 (1) | -0.02 (1) | 0.01(1) |
| | m= 3 | 0.25(1) | 0.17(1) | 0.18 (1) | 0.15 (1) | 0.15(1) |
| | m= -3 | 0.04(2) | 0.03(1) | -0.03 (1) | 0.00 (1) | 0.02(1) |
| Atom | | C(11) | C(12) | C(13) | C(14) | |
| H | l=0,m= 0 | 4.62(3) | 4.70(3) | 4.67 (3) | 4.68 (3) | |
| | l=0,m= 1 | -0.12(1) | -0.12(1) | -0.14 (1) | -0.12 (1) | |
| | m= -1 | 0.00(1) | -0.01(1) | -0.01 (1) | 0.00 (1) | |
| | m= 0 | -0.03(1) | 0.01(1) | 0.01 (1) | -0.02 (1) | |
| | l=2,m= 0 | 0.03(1) | 0.00(1) | 0.00 (1) | 0.06 (1) | |
| | m= 1 | 0.06(1) | 0.01(1) | -0.06 (1) | 0.04 (1) | |
| | m= -1 | 0.01(1) | 0.01(1) | -0.04 (1) | 0.01 (1) | |
| | m= 2 | -0.02(1) | -0.02(1) | 0.04 (2) | 0.01 (1) | |
| | m= -2 | 0.00(1) | 0.00(1) | 0.03 (1) | 0.00 (1) | |
| | l=3,m= 0 | 0.03(1) | -0.03(1) | 0.05 (1) | 0.01 (1) | |
| | m= 1 | -0.10(1) | -0.10(1) | -0.16 (1) | -0.09 (1) | |
| | m= -1 | 0.08(1) | 0.10(1) | 0.06 (1) | 0.10 (1) | |
| | m= 2 | -0.03(1) | -0.05(1) | 0.01 (1) | -0.03 (1) | |
| | m= -2 | -0.04(1) | -0.04(1) | 0.02 (1) | -0.05 (1) | |
| | m= 3 | 0.17(1) | 0.14(1) | 0.11 (1) | 0.16 (1) | |
| | m= -3 | -0.01(1) | -0.01(1) | 0.03 (1) | 0.02 (1) | |
| Atom | | H(1) | H(5) | H(91)-H(113) | H(121)-H(143) | |
| H | l=0,m= 0 | 0.63(2) | 0.61(2) | 0.718(8) | 0.696(8) | |
| | l=0,m= 1 | -0.01(1) | 0.00(1) | -0.007(4) | -0.009(4) | |
| | m= -1 | 0.01(1) | -0.01(1) | -0.015(4) | -0.016(4) | |
| | m= 0 | -0.09(1) | -0.05(1) | -0.020(5) | -0.018(5) | |

Table 4. Agreement Indices of Least Squares Refinements

| | NV | $R_1$ | $R_{1w}$ | $R_2$ | $R_{2w}$ | S |
|---|---|---|---|---|---|---|
| conventional | 127 | 0.0582 | 0.0550 | 0.0794 | 0.0612 | 2.4581 |
| monopole | 146 | 0.0501 | 0.0425 | 0.0653 | 0.0492 | 1.9042 |
| octapole | 368 | 0.0386 | 0.0275 | 0.0429 | 0.0265 | 1.2642 |

$R_1 = \Sigma||F_o|-k|F_c||/\Sigma|F_o|$; $R_{1w} = [\Sigma_w(|F_o|-k|F_c|)^2/\Sigma_w F_o^2]^{1/2}$
$R_2 = \Sigma|F_o^2-kF_c^2|/\Sigma F_o^2$; $R_{2w} = [\Sigma_w|F_o^2-kF_c^2|^2/\Sigma_w F_o^4]^{1/2}$
$S = [\Sigma_w(|F_o|-k|F_c|)^2/(NO-NV)]^{1/2}$
NO = numbers of reflections
NV = numbers of variables

atomic charges obtained from both the multipole refinement and the EHMO method are shown in Fig. 5. From the multipole result, one sees that electron densities are shifted from the H atoms to the carbon atoms. However, from the EHMO result, this shifts are not so evident.

In order to obtain further information about chemical bonding, we carried out a calculation of the deformation density based on the extended Hückel approximation. The molecular geometry was that deduced from the diffraction data; we also tested an idealized geometry with all carbon atoms in the rings in the $sp^2$ configuration. However the slight changes of geometry produced significant effects on neither the orbital energies nor the distribution of deformation density. The theoretical deformation density distribution of the *s*-indacene ring plane is shown in Fig. 6 with the contours defined in Fig. 3. The agreement between the experimental and theoretical deformation density is good except that all the theoretical peak densities are 0.1 - 0.2 e $Å^{-3}$ smaller than the experimental ones. Relative to the density map based on the static multipole model, they are much smaller. The reason is probably that only valence orbitals and electrons are taken into account according to the EHMO method.

Based on the ADP analysis, a transition state of the valence isomerization was proposed.[2] Such a transition state should be consistent firstly with the internuclear distances of the molecule and secondly with the electron density distribution. An extended Hückel calculation was performed on the 1,3,5,7-tetra-R-*s*-indacene, with R = H, $CH_3$ and *t*-butyl assuming the same geometry as the title com-

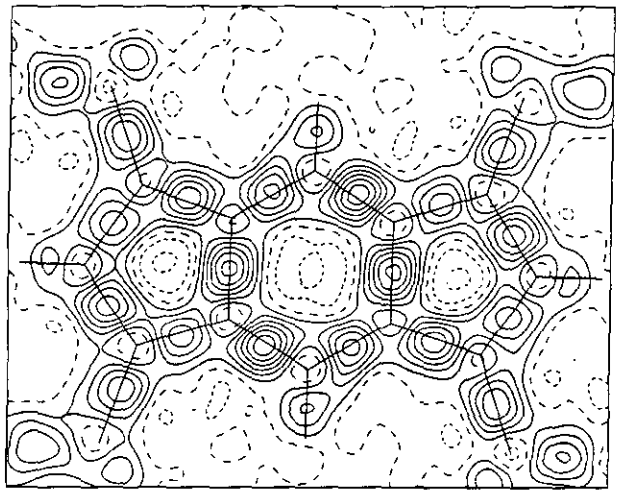

Fig. 3. Experimental deformation density distribution ($\Delta\rho_{x-x}$) of the *s*-indacene plane, with contour level 0.1 e $Å^{-3}$; solid line as positive, dash line zero and dotted line negative.

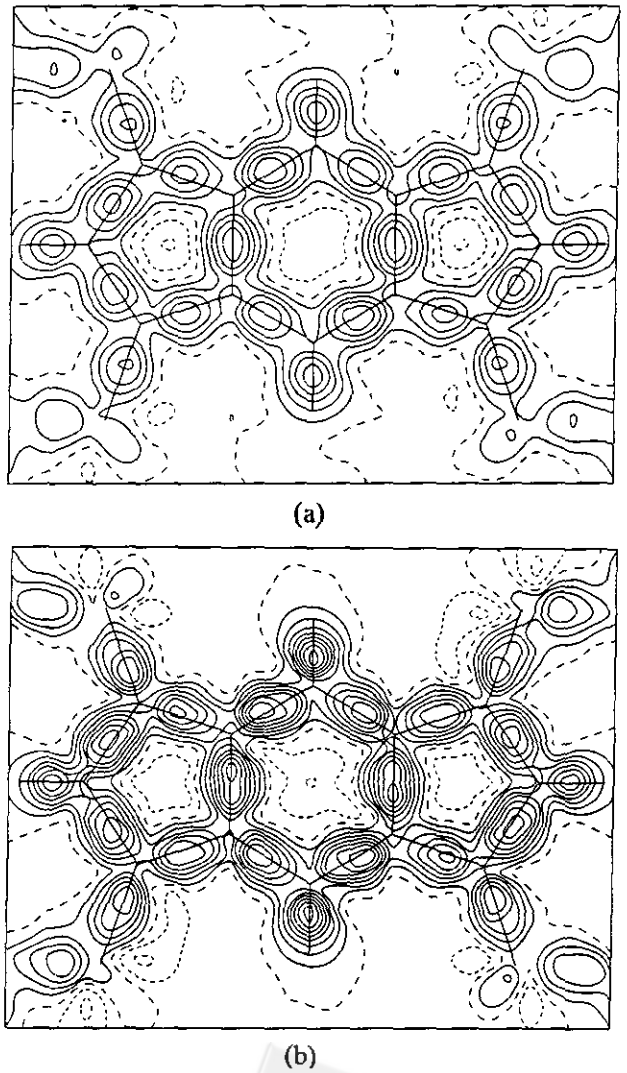

Fig. 4. Multipole deformation density distribution, $\Delta\rho_{M-A}$. (a) dynamic map with the experimental resolution. (b) static map with infinite resolution.

pound. The $\pi$-orbital energies of the three compounds are compared in Fig. 7. Some $\pi$ orbitals of *s*-indacene (R = H) i.e. $B_{1u}$, $B_{3g}$, $B_{2g}$ are evidently split into two on the replacement of H by *t*-butyl, as the substituted carbon atoms take part in the $\pi$ orbitals of the ring. This result may provide the reason for the increase of the thermal stability of such a 12-$\pi$-electron system. However, for the tetra-methyl compound, only $B_{1u}$, $B_{2g}$ orbitals are split, so the effect is not as significant as for the *t*-butyl case. The overall $\pi$-orbital energies are -79.60386, -108.19226, -118.98274 eV for 1,3,5,7-tetra-R-*s*-indacene with R = H, $CH_3$, *t*-butyl respectively. It is also interesting that there are six, eight and nine $\pi$ orbitals respectively; therefore, they correspond to 12, 16 and 18 $\pi$-electron systems. Further results of the $\pi$-bonding system of the title compound are shown in Fig. 8a-i in which all the $\pi$-bonding orbitals are depicted in terms of molecular-orbital contours at 0.5Å above the molecular plane. The nodal planes are clearly shown in the figures: the orbital of least energy ($\pi_1$ - Fig. 8a) exhibits no nodal plane in the ring; $\pi_2$, $\pi_3$, $\pi_5$, $\pi_6$ (Figs. 8b,c,e,f) each exhibits one nodal plane; $\pi_4$, $\pi_7$, $\pi_9$ each (Figs. 8d,g,i) exhibits two nodal planes, and $\pi_8$ (Fig. 8h) has three nodal planes. From the order in energy and the direction of the nodal plane, it seems to indicate that the nodal plane passing through C5, C5* and bisecting C2 - C3, C3* - C2*(horizontal direction) causes a greater increase of orbital energy than that in the vertical direction. It is conceivable that bending out of the plane is easier along the vertical direction than in the

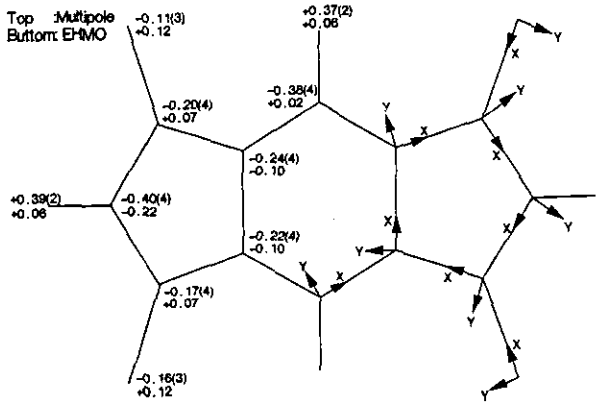


Fig. 5. Net atomic charges obtained from multipole refinement (top) and from EHMO (buttom). Definition local coordinates are also indicated.

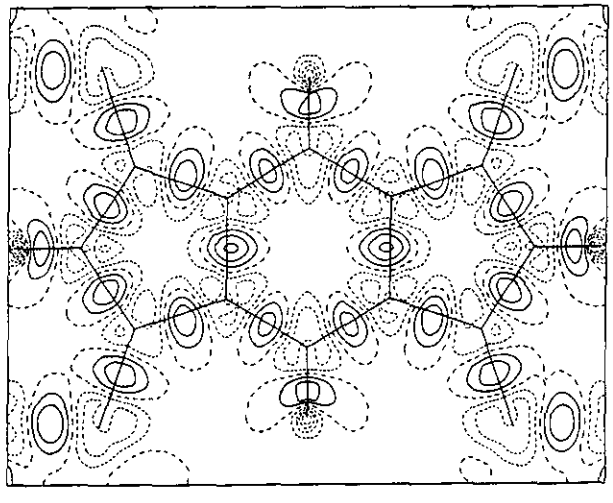

Fig. 6. Theoretical deformation density $\Delta\rho_{theo}$, contours as in Fig. 3.

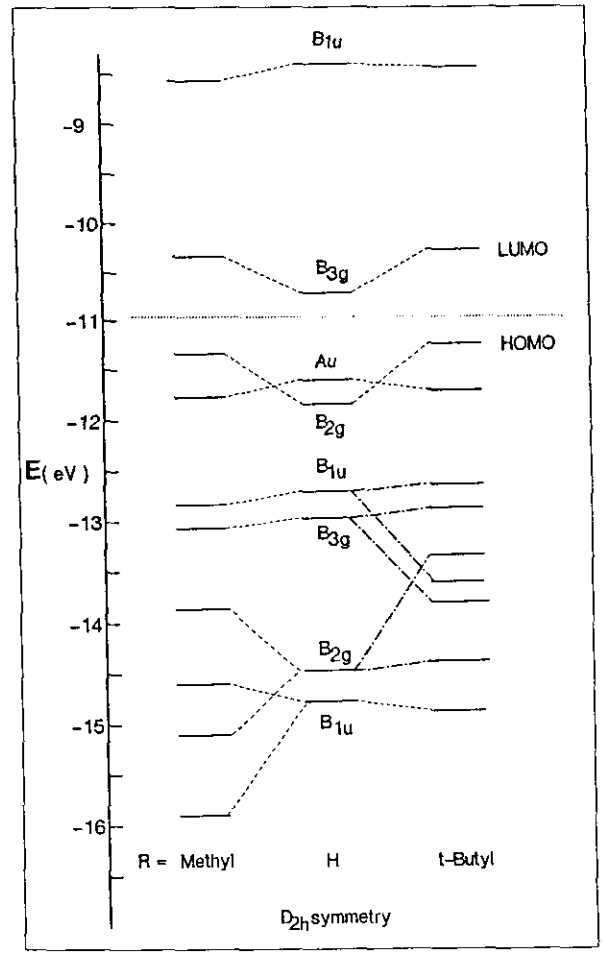


Fig. 7. The orbital-energy level of $\pi$-bonding M.O. for different substituted groups at the 1,3,5,7 positions of *s*-indacene.

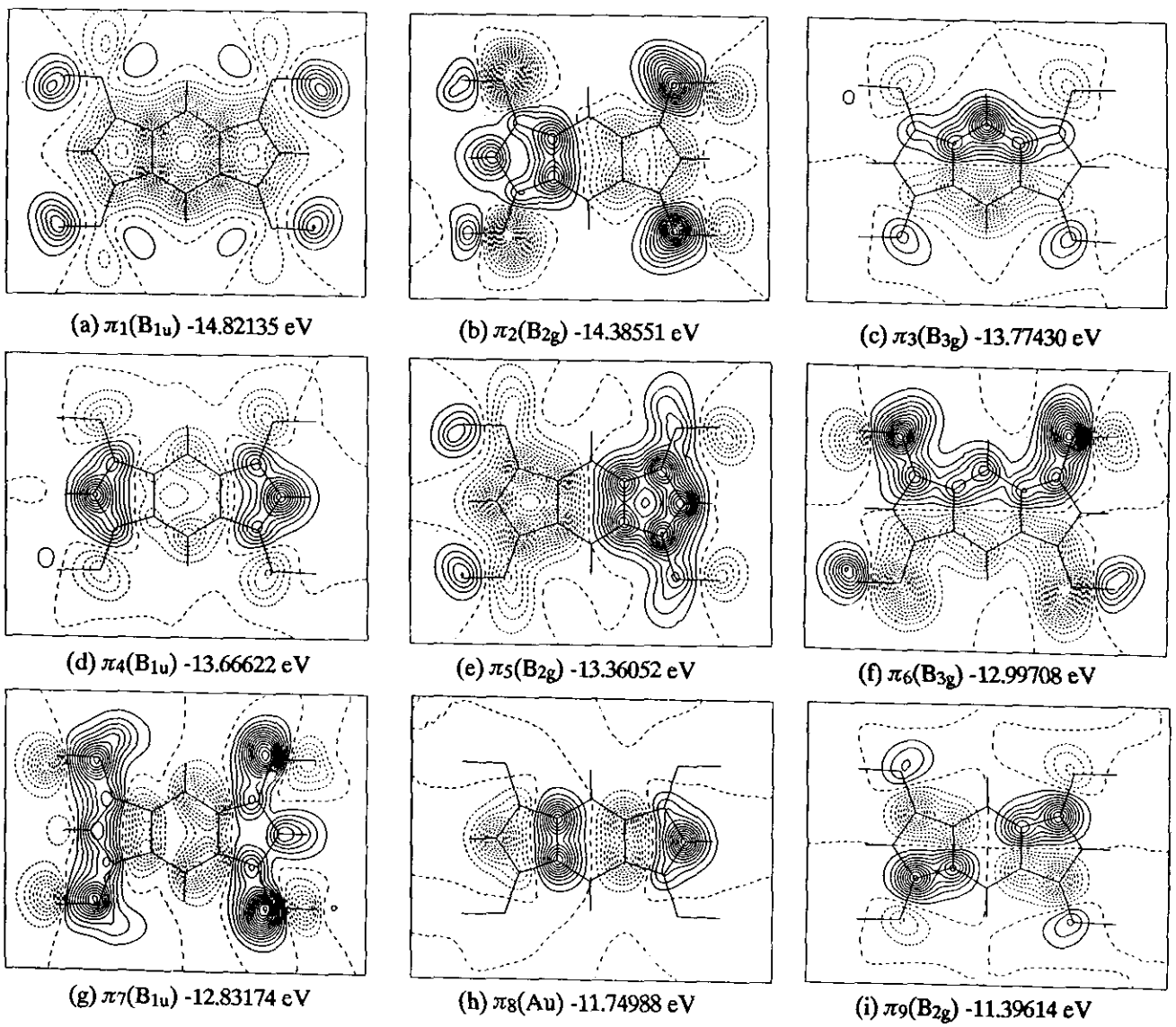


Fig. 8. Nine wavefunctions of the π orbitals of 1,3,5,7-tetra-*t*-butyl-*s*-indacene; positive contour solid, negative dotted.

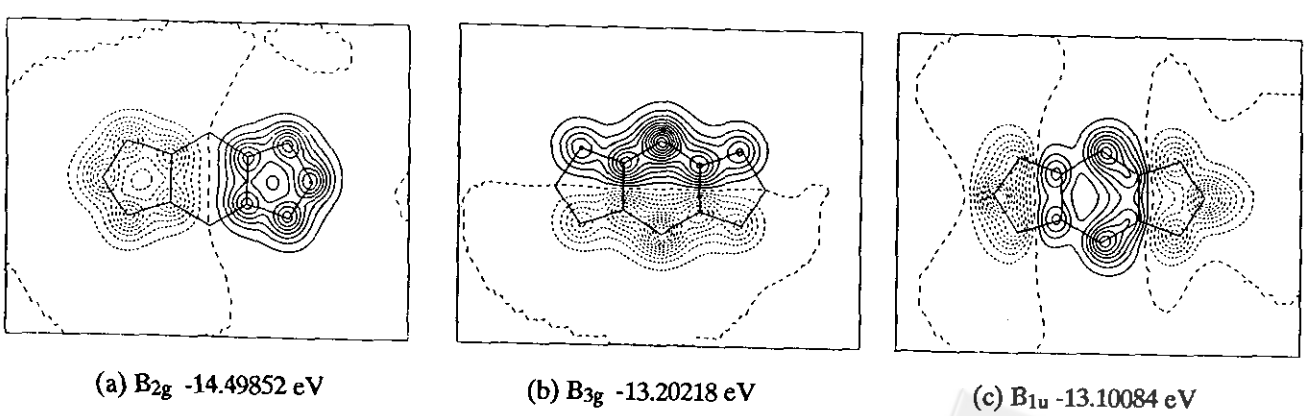


Fig.9. π-Orbital wavefunctions of *s*-indacene which are split into two in tetra-*t*-butyl-*s*-indacene. (a) $B_{2g}$ (b) $B_{3g}$ (c) $B_{1u}$, contour as in Fig. 8.

horizontal direction. This result agrees with the observations of the ADP analysis.[2] Among them, six $\pi$ orbitals ($\pi_2$, $\pi_5$; $\pi_3$, $\pi_6$; $\pi_4$, $\pi_7$ - Figs. 8b,e,c,f,d,g) originate from three $\pi$-orbitals in *s*-indacene ($B_{2g}$, $B_{3g}$ and $B_{1u}$ - Figs. 9a,b,c). The reason is that the occupied $\pi$ orbitals are further coupled with the central carbon atom of the *t*-butyl groups at the 1,3,5,7-positions and split into two levels with different signs on the substituted carbon atoms e.g. Fig. 9a. vs. Figs. 8b,e. These extra orbitals contribute to the bonding of C1-C2; C4-C5; C5-C6 and antibonding of C2-C3 and C2-C6. These results are consistent with our experimental bond distances. Also, in the $B_{1u}$ mode (Figs. 9c and 8d,f), clearly there are two nodal planes between atoms C2,C6/C3,C4 and C2*,C6*/C3*,C4* which make the bending of C4-C5-C6 and C4*-C5*-C6* parts accessible. Moreover, the-out-of plane thermal motion is much greater than the rigid-body motion for C5 ($\Delta u \cong 59pm^2$).[2] Thus the $B_{1u}$ mode certainly fits the out-of-plane motion of C4-C5-C6. Any vibrational mode in resonance with such a wavefunction could yield a slightly bent geometry which was proposed as the transition state of this molecule[2] in the solid state. As for the electron density distribution, all the C-C bonds are about the same within 0.1 e $Å^{-3}$. Hence the differences of the electron density may not be as clear as those of the distances, partially because the comparison of bonds should be made on the integration of the density between the bonded atoms rather than the peak density, as the density distribution is a shape-dependent function. Even after integration, the standard deviation may make the comparison meaningless.

## CONCLUSION

From the bond lengths, analysis of anisotropic thermal motion and results on the deformation density of the substituted *s*-indacenes, the title compound can certainly be described as neither the resonance between two valence isomers (**1A** and **1B**), nor the delocalized model (**1C**); it is probably best described as **1D**. This description would make the C4-C5-C6 part easy to bend out of the ring plane. From the analyses of the nine occupied $\pi$-bonding wavefunctions, there are three orbitals ($\pi_4$, $\pi_7$, $\pi_8$) which contribute directly to such a form. The stabilization of such a 12-$\pi$-electron system(*s*-indacene) by the bulky *t*-butyl groups can be realized as a 18 $\pi$-electron system, because of the contribution from the substituted carbon atoms.

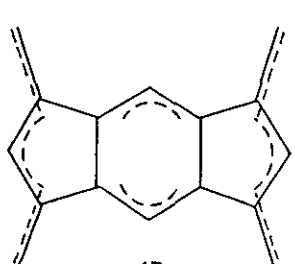

1D

Although most theoretical deformation density studies have been based on ab-initio[11-13] calculation or a local density functional method,[14-16] our results indicate that for molecules containing only light atoms, EHMO can also provide a valid comparison, especially on the delocalized $\pi$-bonding system.

## ACKNOWLEDGMENT

The authors thank Dr. C. Krüger and Mr. K. H. Claus for their assistance with diffraction data measurements and the National Science Council of ROC for financial support.

Received September 26, 1990.

**Key Words**

Deformation density distribution; *s*-Indacene.

## REFERENCES

1. Hafner, K.; Stowasser, B.; Krimmer, H. P.; Fischer, S.; Bohm, M. C.; Lindner, H. J. *Angew. Chem. Int. Ed.*, **1986**, *25*, 630; *Angew. Chem.* **1986**, *98*, 646.
2. Dunitz, J.; Krüger, C.; Irngartinger, H.; Maverick, E.; Wang, Y.; Nixdorf, M. *Angew. Chem. Int. Ed. Engl.*, **1988**, *27*, 387. *Angew. Chem.*, **1988**, *100*, 415.
3. Wang, Y.; Angermund, K.; Goddard, R.; Krüger, C. *J. Am. Chem. Soc.* **1987**, *109*, 587.
4. Both ICON and MOPLOT programs are from QCPE, Department of Chemistry, Indiana University, Bloomington, Indiana 47405, U.S.A.
5. Tsai, C. J.; 1982, Master thesis, National Taiwan Univ.
6. Hansen, N.; Coppens, P. *Acta. Cryst.*, **1978**, *A34*, 909.
7. Positional parameters from full data refinement are also in Cambridge data base.
8. (a) Wang, Y.; Tsai, C. J.; Liu, W. L.; Calvert, L. D. *Acta.*

*Cryst.* **1985**, *B41*, 131-135. (b) Coppens, P.; Dam, J.; Harkema, S.; Feil, D.; Feld, R.; Lehmann, M. S.; Goddard, R.; Krüger, C.; Hellner, E.; Johansen, H.; Larsen, F. K.; Koetzle, T. F.; Mcullan, R. K.; Maslen, E. N.; Stevens, E. D. *Acta. Cryst.* **1984**, *A40*, 184.

9. Wang, Y.; Chen, M. J.; Wu, C. H. *Acta. Cryst.* **1988**, *B44*, 179.
10. Wang, Y.; Liao, J. H. *Acta. Cryst.* **1989**, *B45*, 65.
11. Kunze, K. L.; Hall M. B. *J. Am. Chem. Soc.*, **1987**, *109*, 7617.
12. Johansen, H. *J. Am. Chem. Soc.* **1988**, *110*, 5322.
13. Rohmer, M. *Inorg. Chem.* **1989**, *28*, 4574.
14. Fabius, B.; Cohen-Addad, C.; Larsen, F. K.; Lehmann, M. S, Becker, P. *J. Am. Chem. Soc.* **1989**, *111*, 5728.
15. Velders, G. J. M.; Feil, D. *Acta. Cryst.* **1989**, *B45*, 359.
16. Moeckli, P.; Schwarzenbach, J. *Acta. Cryst.* **1988**, *B44*, 636.